Measuring Zenith Sky Brightness and Color Changes during the April 8, 2024 Total Solar Eclipse Using Filtered Sky Quality Meters

Jennifer Birriel
Brayden Schwegman
Ivan Hargesheimer
Department of Engineering Sciences, Morehead State University, 150 University Boulevard, Morehead, KY 40351; j.birriel@ moreheadstate.edu

Received September 15, 2025; revised January 26, 2026; accepted January 27, 2026

Abstract Zenith sky brightness measurements were obtained on the line of totality during the April 8, 2024, total solar eclipse. Observations were made at two sites: Wickliffe, Kentucky, and Oxford, Ohio. A set of four Sky Quality Meters (SQMs) fitted with clear (L), red (R), green (G), and blue (B) filters collected data at each site. During totality, sky brightness dropped to 13.27 ± 0.1 mag/arcsec^2 at Wickliffe, Kentucky, and 12.99 ± 0.1 mag/arsec^2 at Oxford, Ohio. These values are consistent with past eclipse observations and are brighter than nautical twilight. Over the course of the partial eclipse the spectral content prior to totality, as measured by the R–B and G–B indices, remained constant. During totality, the spectral content shifted towards B, consistent with the light arriving at zenith from outside the umbra after multiple scattering events. The spectral content of zenith sky brightness post-totality decreased at a constant rate due to changes in solar altitude. The use of color-filtered SQMs greatly simplifies the data collection process with regards to both photometric and spectrophotometric measurements.

1. Introduction

During a total solar eclipse, the disk of the Sun is covered by the disk of the Moon, and the sky darkens; however, this darkness does not rival that of the night sky due to the presence of sunlight scattered by the atmosphere from regions outside of totality. Photometric measurements of zenith sky brightness have been conducted for the past hundred years or so, while a handful of spectrophotometric measurements have been made only over the last sixty years or so (Sharp *et al.* 1966; Hall 1971; Shaw 1975; Silverman and Mullen 1975; Kirilov *et al.* 2001; Suzuki and Yamamoto 2013; Shaw *et al.* 2022). Previous total eclipse observations have established several photometric and spectrophotometric characteristics: (a) Zenith during totality is 10^{-3} times that of a normal daytime sky while a full moon at night is 10^{-6} times that of normal daytime brightness. (b) Sky brightness at zenith is a linear function of solar obscuration up to 99.8% coverage. (c) The spectral signature of the sky shifts towards the blue from about a minute before to about a minute after totality. (d) Local effects including atmospheric conditions and solar elevation angle become important near and during totality.

Theoretical models for sky brightness and color during total solar eclipses employ first- and second-order Rayleigh scattering processes (Gedzelman 1975; Shaw 1975). Both models qualitatively agree with observations of a reddened horizon and blue enrichment at zenith. Gedzelman (1975) confined his work to modeling sky conditions near the horizon. Shaw (1978) modeled the full sky; his work predicted a zenith spectral radiance in blue that was 20% lower than that observed during the 1973 total eclipse observed from Africa. More recently, Shaw *et al.* (2022) utilized the 1975 Shaw model with a calibrated all-sky image at totality during the 2017 eclipse. Their predicted and measured brightnesses agreed to within a factor of 2. Refinement of atmospheric scattering models during total solar eclipses should be possible with additional data from spectrophotometric measurements and all-sky imaging during solar eclipses.

The total solar eclipse of April 8, 2024, stretched across North America. The line of totality ran from southern Canada through 13 U. S. states (Maine, New Hampshire, Vermont, New York, Pennsylvania, Ohio, Indiana, Illinois, Kentucky, Missouri, Arkansas, Oklahoma, and Texas) and across central Mexico. We present photometric measurements in the L, R, G, B bands at two different sites in America: Wickliffe, Kentucky, and Oxford, Ohio. At both sites, the skies had passing clouds for about an hour before and after totality; visibility was good at both sites and recorded to be approximately10 miles, according to archival data from timeanddate.com (Time and Date AS. 1995–2026).

2. Instrumentation

Prior to 2016 sky brightness measurements were primarily obtained using photoelectric photometers and spectroscopes (Sharp *et al.* 1966; Hall 1971; Silverman and Mullen 1975).

During the 2017 total solar eclipse, Shaw *et al.* (2022) utilized a radiometrically calibrated all-sky camera to examine sky brightness and color in the R, G, B bands. Two groups (Pramudya and Arkanuddin 2016; Wijaya *et al.* 2016) used SQMs to measure sky brightness at zenith during the 2016 total solar eclipse.

There are several Unihedron SQM models and all designed to measure night sky brightness at zenith in magnitudes per arcsecond squared (mpsas). This study used the SQM-L-DL model which has data logging capabilities and is powered by six 1.5-V batteries. SQM-L models include a lens that narrows the acceptance angle of the device to a 20-degree cone around zenith. The SQM uncertainty for any individual measurement is ± 0.1 magnitude per square arcsecond (mpsas), as stated by

the manufacturer. Thus, comparing the difference between any two SQMs measurements results in an experimental uncertainty of ± 0.14, using the addition of errors in quadrature. Full technical specifications and performance of the SQM-L models are available from Cinzano (2005).

We constructed two identical devices to measure zenith sky brightness. Each device consisted of four SQM-L-DL units in protective housing. Each individual SQM-L-DL was fitted with a single color filter: either an clear (L), red (R), green (G), or blue (B) filter. We used the 1.25-inch LRGB filter set from ZWO Astro (2026).Observations at each site were made starting about an hour before the eclipse began and continued for roughly an hour after totality.

Measurements for each device are corrected for extinction of light from the glass window on the weatherproof housing as well as detector response and transmission losses from its respective L, R, G, B filter. Each color filter has nominally uniform transmission of approximately 92% along its bandpass. Spoelstra (2014) used SQMs with color filters to monitor night sky brightness and we are using a device similar to his, so we employ his method to determine our correction factors. The reading from a spectral band depends on the SQM detector response and the filter transmission. The true light level measured by our device is given in Equation 1:

$$m_{corrected} = m_{reading} - 2.5 \log (1/R_{band}), \quad (1)$$

Here R_{band} is the average response in the spectral band. It is calculated by taking the sum of the detector response at each wavelength λ multiplied by the filter transmission T_λ in each wavelength interval Δ_λ and dividing by the number of wavelength intervals. This is given in Equation 2 by

$$R_{band} = (\text{Sum } (R_{detector\lambda T\lambda})/n_{\Delta\lambda}. \quad (2)$$

The correction factors for each filter are listed in Table 1.

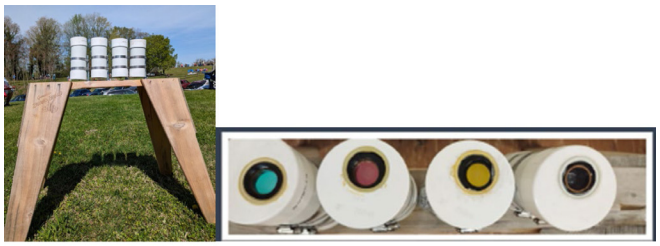

(a) (b)

Figure 1. (a) Bank of SQM-L-DL devices in weatherproof housing and mounted on a sawhorse viewed from the side. (b) A view from the top with filters visible, from left to right: Red (R), Green (G), Blue (B), and clear or luminous (L).

Table 1. Corrections for SQM response and RGB filter transmission.

Filter Color	*Wavelength Band (nm)*	*Color Wavelength (nm)*	*Correction Factors* R_{band} *(%)*	$-2.5 \log (1/R_{band})$ *(mag/arcsec²)*
Red	600–680	640	93	–0.08
Green	500–550	525	77	–0.29
Blue	411–470	440	59	–0.58

3. Results and discussion

3.1. Zenith sky brightness

Measurements were made at two sites along the line of totality: the details for each site are found in Table 2. The SQM-L-DL with the clear (L) filter is saturated until roughly 10 minutes prior to totality at either site, as see in Figure 2; the device is known to have a saturation threshold of 5.9 mpsas. The vertical dotted lines from left to right indicate the predicted times of C2 (start of totality), C3 (end of totality), and C4 (end of partial eclipse). Note that there is a slight discrepancy between predicted and measured times, probably because the SQM clocks were not synchronized with local atomic time.

Table 2. Sites and eclipse characteristics (timeanddate.com).

	Oxford, Ohio	*Wickliffe, Kentucky*
Latitude and Longitude	39.51° N, 84.75° W	37.05° N, 88.94° W
Time Zone	EDT	CDT
Length of Eclipse	$2^h\ 30^m$	$2^h\ 36^m$
Length of Totality	$3^m\ 53^s$	$2^m\ 46^s$
C1 Local Time	13:57:39	12:42:00
C1 Solar Altitude	55.8°	60.2°
C2 Local Time	15:12:13	13:59:18
C2 Solar Altitude	49.6°	57.5°
Maximum Local Time	15:14:10	14:00:41
Maximum Solar Altitude	49.4°	57.4°
C3 Local Time	15:16:06	14:02:04
C3 Solar Altitude	49.1°	57.1°
C4 Local Time	16:27:52	15:17:52
C4 Solar Altitude	38.8°	149.6°

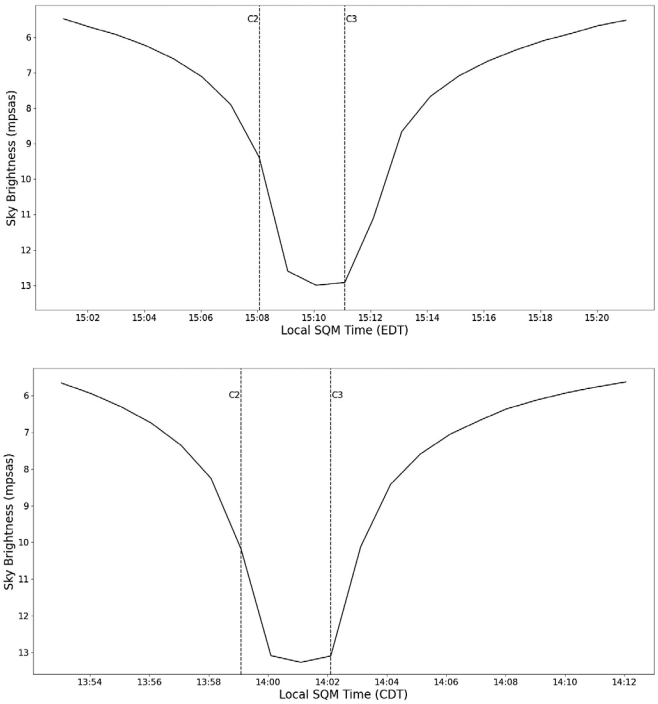

Figure 2. Zenith sky brightness as measured by an SQM with a clear (L-band) filter. Times are in local daylight savings: EDT for Oxford, Ohio, (top) and CDT for Wickliffe, Kentucky, (bottom). Predicted times of C2 and C3 are indicated by the vertical dashed lines: the discrepancy is likely due to SQM clocks not being synchronized to local atomic time.

The darkest measurement of zenith sky brightness for each site occurs during maximum eclipse or mid-totality. At Oxford, Ohio, this was 12.99 ± 0.1 mpsas and 13.27 ± 0.1 mpsas for the Wickliffe, Kentucky, site. These values are consistent with SQM measurements for the March 9, 2016, eclipse: 12.88 mpsas (Wijaya, *et al.* 2016) and 12.47 mpsas (Pramudya and Arkanuddin 2016). Zenith sky brightness at maximum eclipse is slightly brighter than zenith sky brightness of nautical twilight, which is between 13.68 and 13.94 mpsas (Schmude 2024).

3.2. Planetary visibility and zenith brightness

Venus and Jupiter were clearly visible to the naked eye during totality: see Figure 3, which was produced using Stellarium online software (Stellarium Web 2026). When looking southward, Jupiter (magnitude –1.89) appeared roughly 30 degrees to the upper left of the eclipsed Sun and Venus (magnitude –3.78) was located about 15 degrees to lower right of the eclipsed Sun. Mars (magnitude 1.17) and Saturn (magnitude 1.14) were difficult to spot with the naked eye.

Planetary visibility during the eclipse can be determined using the relationship derived by Fisher (2006) which relates sky brightness to naked eye limiting magnitude (NELM). The relationship between NELM and sky brightness B (in mpsas) is given in Equation 3 by

$$\mathrm{NELM} = 7.93 - 5 * \log\left(10^{((4.316 - B/5) + 1)}\right) \quad (3)$$

At Oxford, Ohio, where B = 12.99, the NELM was –0.70, while at Wickliffe, Kentucky, with B = 13.27, the NELM was –0.43. At both sites, Saturn and Mars were well below the threshold of naked eye visibility while both Venus and Jupiter were much brighter than the naked eye threshold.

3.3. Zenith sky color

Measurements of sky brightness in the red (R), green (G), and blue (B) were obtained at each site (see Figure 4). During totality, red light is attenuated to a greater extent than blue or green. This is consistent with Rayleigh scattering: most of the light making it to zenith during totality represents light from outside the umbral shadow that has been scattered multiple times.

Spectral changes are revealed by taking the color index B–R for our data (Sharp *et al.* 1966; Silverman and Mullen 1975). A larger negative number for these differences translates to an excess of blue. As seen in Figure 5, both sites show a nearly constant color ratio between R and B until totality, consistent with previous studies (Hall 1971; Sharp *et al.* 1966). It is clear from these plots that during totality, the ratio of blue light increases relative to red light as would be expected if multiply-scattered photons reach zenith from outside the umbral shadow. After totality, the relative intensities of red and blue decrease with decreasing solar altitude.

4. Concluding remarks

We have several recommendations for future SQM observations of total solar eclipses. First, the SQM data collection rate should be reduced to a 10-second interval to improve resolution during totality. Second, the green-filtered SQM can be eliminated as it offers little additional information: the L, R, B filters are sufficient to measure sky brightness and spectral content. Finally, it is desirable to synchronize SQMs with local atomic time if accurate timing of C2 and C3 are desired. There is currently a dearth of such measurements made during total solar eclipses. Such measurements would be useful to inform scattering models (Shaw *et al.* 2022;

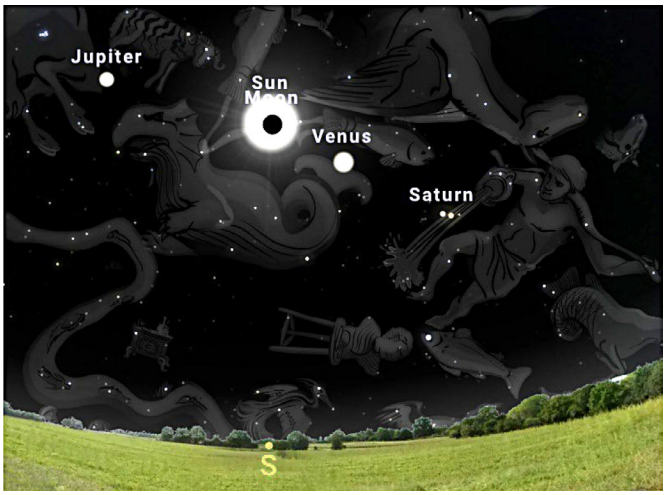

Figure 3. Planets near the eclipsed sun. Only Jupiter and Venus were easily visible to the naked eye. This image is a view directly south at totality. Saturn is the yellow dot and Mars is the smaller, red object immediately to its right. This was produced using Stellarium online software (https://stellarium-web.org).

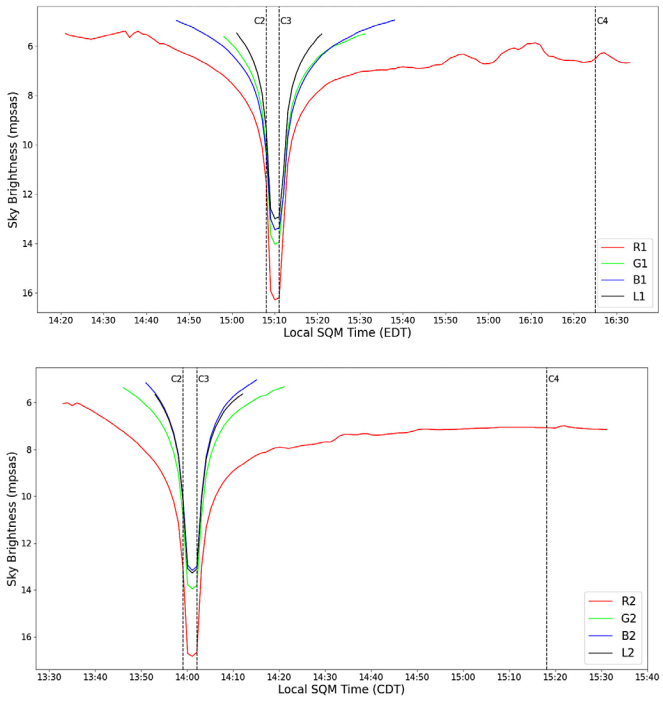

Figure 4. Zenith brightness at Oxford, Ohio, (top) and Wickliffe, Kentucky, (bottom), measured by SQMs with red, green, and blue filters. Note that the red light shows greater extinction during totality than both blue and green. Note that green and blue are quite close in magnitude and the relative intensities are flipped at both sites. This discrepancy is probably due to a combination of experimental uncertainty and local and geometric effects (Silverman and Mullen 1975).

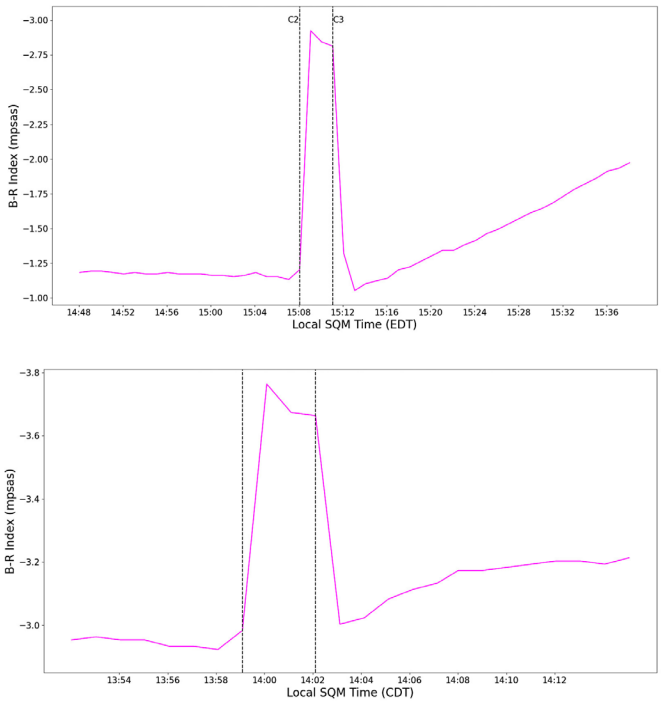

Figure 5. Spectral content around totality measured by color index B–R. Prior to totality, the spectral content is constant. After totality, the ratio decreases linearly with decreasing solar altitude. During totality the deficit of red light compared to both blue and green is what would be expected if light arriving at zenith is primarily from multiply scattered photons from outside the umbral shadow.

Shaw 1975). As mentioned by Hall (1971) comparison of results from different measurements is complicated by instrumental factors including calibration and type of instrument used. The use of SQMs and filters with known properties could provide a standardized measurement system that would simplify comparison of future eclipse observations at different locations and dates. The use of SQMs greatly reduces the complexity of setup and data reduction and researchers currently in possession of SQMs can contribute to such studies.

5. Acknowledgements

The authors wish to thank Morehead State University's Undergraduate Research Fellowship program for providing financial support B. Schwegman and I. Hargesheimer. They also thank the anonymous referee for suggestions that improved the quality and clarity of this paper.

References

Cinzano, P. 2005, *ISTIL Internal Rep. No. 9*, **1.4**, 1.
Fisher, K. 2006, Conversion Calculator.[1]
Gedzelman, S. D. 1975, *Appl. Opt.*, **14**, 2831.
Hall, W. N. 1971, *Appl. Opt.*, **10**, 1225.
Kirilov, K., Angelova, E., Popov, G., Umlenski, V., Avramov, L., and Tsanev, V. 2001, *Comptes Rendus Acad. Bulgare Sci.*, **54**, 49.
Pramudya, Y., and Arkanuddin, M. 2016, *J. Phys. Conf. Ser.*, **771**, 012013.
Schmude, R. 2024, *Georgia J. Sci.*, **82**, 106.
Sharp, William E., Lloyd, J. W. F., and Silverman, S. M. 1966, *Appl. Opt.*, **5**, 787.
Shaw, G. E. 1975, *Appl. Opt.*, **14**, 388.
Shaw, G. E. 1978, *Appl. Opt.*, **17**, 272.
Shaw, J. A., Shaw, G. E., Scherrer, B., Eshelman, L. M., and Turcotte, S. 2022, *Proc. SPIE*, 12214, 1221403-1.
Silverman, S. M., and Mullen, E. G. 1975, *Appl. Opt.*, **14**, 2838.
Spoelstra, H. 2014, *J. Quant. Spectrosc. Radiat. Transfer*, **139**, 82.
Stellarium Web. 2026, Stellarium online software (https://stellarium-web.org).
Suzuki, H., and Yamamoto, A. 2013, *Earth Moon Planets*, **110**, 157.
Time and Date AS. 1995–2026, "timeanddate" (https://www.timeanddate.com).
Wijaya, A. F. C., *et al.* 2016, *J. Phys. Conf. Ser.*, **771**, e012012.
ZWO Astro. 2026, "Filters & Filter Wheels," ZWO Astro USA (https://us.zwoastro.com/collections/filters-_and_filter_wheels).

[1] Fisher (2006): https://www.unihedron.com/projects/darksky/NELM2BCalc.html